Interferon γ Regulates Platelet Endothelial Cell Adhesion Molecule 1 Expression and Neutrophil Infiltration into Herpes Simplex Virus–infected Mouse Corneas

By Qizhi Tang* and Robert L. Hendricks*‡§

*From the Departments of *Microbiology and Immunology ‡Ophthalmology and Visual Sciences, and §Pathology, University of Illinois at Chicago, Chicago, Illinois 60612*

Summary

In a mouse model of herpes simplex virus (HSV) 1 corneal infection, tissue destruction results from a $CD4^+$ T cell–mediated chronic inflammation, in which interleukin 2 and interferon (IFN)γ are requisite inflammatory mediators and polymorphonuclear leukocytes (PMN) are the predominant infiltrating cells. In vivo neutralization of IFN-γ relieved inflammation at least in part through a specific block of PMN extravasation into HSV-1-infected corneas. Intercellular adhesion molecule (ICAM) 1 and platelet endothelial cell adhesion molecule (PECAM) 1 were upregulated on the vascular endothelium of inflamed corneas. Reduced PMN extravasation in anti–IFN-γ–treated mice was associated with a dramatic reduction of PECAM-1 but not ICAM-1 expression on vascular endothelium. PMN accumulated in the lumen of corneal vessels after in vivo IFN-γ neutralization. PECAM-1 was readily detectable on PMN inside the vessels but was not detectable on PMN that extravasated into the infected cornea. Moreover, flow cytometric analysis revealed reduced PECAM-1 expression but elevated major histocompatibility complex class I expression on PMN that recently extravasated into the peritoneal cavity when compared with PMN in the peripheral blood. We conclude that IFN-γ contributes to HSV-1–induced corneal inflammation by facilitating PMN infiltration; this appears to be accomplished through upregulation of PECAM-1 expression on the vascular endothelium; and PMN downregulate PECAM-1 expression during the process of extravasation.

In infectious diseases, inflammation can contribute to the elimination or control of the infectious agent. However, in some cases, inflammation can become chronic and result in the destruction of healthy tissue. In general, these chronic inflammatory responses are immunologically mediated. In our mouse model of HSV-1 corneal disease, primary infection is followed by the appearance within 2 d of epithelial lesions that heal by 4 d after infection. The lesions are characterized by the presence of replicating virus in the corneal epithelium (1). Resolution of the epithelial lesions is followed by a clinically quiescent period of ~1 wk. At that time, ~50% of the infected corneas develop a chronic inflammation that results in progressive destruction of the corneal architecture. It is this chronic inflammation in the corneal stroma that is associated with visual morbidity in human patients suffering from HSV keratitis.

The corneal stromal inflammation resulting from infection of mice with the RE strain of HSV-1 is characterized by an inflammatory infiltrate comprised predominantly of PMN and $CD4^+$ T lymphocytes. This inflammatory response is abrogated by in vivo depletion of $CD4^+$ T lymphocytes (2). The Th1 cytokines IL-2, IFN-γ, and TNF-α/β, but not Th2 cytokines IL-4 and IL-10, are detected in leukocytes extracted from inflamed corneas after HSV-1 infection (3). Moreover, studies from our laboratory demonstrated that neutralizing the Th1 cytokines IL-2 or IFN-γ, but not the Th2 cytokine IL-4, can prevent the inflammation from developing (4). Although Th2 cytokines have not been detected in HSV-1–infected corneas, they may play a protective role when given exogenously. For instance, a recent study demonstrated that combined intracorneal and systemic injection of IL-10 before HSV-1 infection significantly suppressed corneal inflammation (5). These findings suggest that a Th1 $CD4^+$ T lymphocyte response to HSV-1 antigens in the infected cornea regulates the infiltration and/or tissue-destructive functions of PMN.

IFN-γ possesses a number of proinflammatory characteristics. These include upregulation of MHC expression, activation of cytokine secretion, phagocytosis, and production of reactive oxygen and nitrogen intermediates by macrophages (for reviews see references 6–8). In our mouse model of HSV-1 corneal infection, the inflammatory infiltrate during active disease consists largely of T cells and PMN. Macrophages infiltrate the cornea late in the inflammatory process, and thus appear to be primarily involved in the resolution of the inflammatory response. Therefore, proinflammatory functions of IFN-γ that are mediated through macrophages may not contribute substantially to

 J. Exp. Med. © The Rockefeller University Press • 0022-1007/96/10/1435/13 $2.00
Volume 184 October 1996 1435–1447

the tissue destruction associated with this disease. IFN-γ has also been shown to activate PMN and vascular endothelial cells (9–16). The effects of IFN-γ on vascular endothelium include increased expression of adhesion molecules that contribute to PMN extravasation. However, most of the proinflammatory functions of IFN-γ were established in vitro and require confirmation in clinically relevant models of inflammation in vivo.

In our mouse model of HSV-1–induced corneal inflammation, T cells are not required to control HSV-1 replication in the cornea, and in fact contribute to corneal tissue destruction and visual morbidity. Thus, this model offers an opportunity to manipulate T cell–mediated inflammation without the complication of pathologic changes resulting from uncontrolled virus replication. In this study, we have used this model to investigate the proinflammatory functions of IFN-γ in vivo.

Materials and Methods

Ocular HSV-1 Infection and Evaluation of Corneal Inflammation. The RE strain of HSV-1 was grown in Vero cells, and intact virions were purified on Percoll (Pharmacia Biotech Inc. Piscataway, NJ) as previously described (17). Female A/J mice (Frederick Cancer Research and Development Center, Frederick, MD) 6–8 wk of age were anesthetized by intramuscular injection of 2 mg of ketamine hydrochloride (Phoenix Scientific, Inc., St. Joseph, MO) and 0.04 mg of acepromazine maleate (Aveco Co., Fort Dodge, IA) in 0.1 ml of HBSS. Corneas of anesthetized mice were scarified 10 times in a crisscross fashion with a sterile 30-gauge needle, and the eyes were infected topically with 3 μl of RPMI containing 10^5 plaque-forming units of HSV-1. Mice were treated with gentamicin (Genoptic; Allergen America, Puerto Rico) topically from day 4 to day 11 after infection to prevent bacterial superinfection.

Corneal stromal opacity resulting from inflammatory cell infiltration was evaluated by daily slit-lamp examination after infection as previously described (1, 2). The opacity was scored by an observer who was unaware of the treatment given using the following scale: 1+ = mild haziness; 2+ = moderate opacity not obscuring the view of the iris; 3+ = severe opacity in which iris details are no longer visible; 4+ = corneal perforation.

Antibodies and Cytokines. A rat anti–mouse IFN-γ mAb (R4-6A2; American Type Culture Collection, Rockville, MD) was used for in vivo neutralization. In some experiments, a rat anti–HLA-DR5 mAb (SFR3-DR5; American Type Culture Collection) was used as an antibody control, and a rat anti–IL-2 mAb (S4B6; American Type Culture Collection) was used as a specificity control. The anti–HLA-DR5 mAb does not bind detectably to any mouse tissue. All three antibodies were purified from hybridoma culture supernatant by affinity chromatography on protein G–Sepharose Fastflow (Pharmacia Biotech) and quantified with a radial immunodiffusion kit (ICN Biomedicals; Costa Mesa, CA). For immunohistochemistry, anti–intercellular adhesion molecule (ICAM)[1] 1 (YN/17.4), anti–Mac-1 (M1/70), and anti–LFA-1 (M17/4.2) mAbs, all obtained from American Type Culture Collection, were purified from hybridoma culture medium and biotinylated using an immunoprobe biotinylation kit (Sigma Chemical Co., St. Louis, MO). The biotinylated anti–mouse platelet endothelial cell adhesion molecule (PECAM) 1 mAb (MEC 13.3) and anti-CD3 (145-2C11) were purchased from PharMingen (San Diego, CA). Anti–mouse granulocyte mAb (RB6-8C5, provided by R. Coffman, DNAX Research Institute, Palo Alto, CA) was isolated from hybridoma culture medium and conjugated to FITC using standard procedures. A rat mAb specific for a nonpolymorphic region of mouse MHC class I (M1/42.3.9.8) was obtained from American Type Culture Collection, purified from hybridoma supernatant as described above, and used in conjunction with a FITC-conjugated goat anti–rat IgG (H + L) (Jackson ImmunoResearch Laboratories, Inc., West Grove, PA) in an indirect staining procedure. Mouse rIFN-γ was purchased from Genzyme Corp. (Cambridge, MA).

Histologic and Immunohistologic Examination. Inflamed eyes were excised at different times after mAb treatment, fixed in 10% neutral buffered formalin, and 5-μm paraffin sections were prepared. The sections were stained with hematoxylin and eosin (H&E), mounted with Permount, and coverslipped for microscopic examination. For immunohistochemical staining, eyes were embedded in OCT compound (Optimal Cryogenic Temperature; Miles, Inc., Elkhart, IN), snap-frozen immediately in an isopentane–dry ice bath, and 6-μm sections were cut at −20°C. Sections were fixed with acetone for 10 min and blocked with PBS-BGEN (3% BSA, 0.25% gelatin, 5 mM EDTA, 0.025% NP-40) for 20 min, and then processed for immunofluorescence or immunoperoxidase staining. For immunoperoxidase staining, sections were incubated with biotinylated antibodies for 1 h at 37°C. Cells with bound antibodies were identified with a peroxidase reagent (Elite Vectastain ABC; Vector Laboratories Inc., Burlingame, CA) using a diaminobenzidine peroxidase substrate kit (Vector Laboratories, Inc.). For two-color immunofluorescence staining, sections were then incubated for 1 h with a mixture of 0.5 μg/ml of FITC-labeled anti–mouse granulocyte mAb (RB6-8C5) and 4 μg/ml of biotinylated anti–mouse PECAM-1. The sections were then washed and incubated with 0.6 μg/ml of PE-conjugated streptavidin (PharMingen) for 30 min. Slides were then washed, mounted with Permafluor (Lipshaw, Detroit, MI), and coverslipped.

Evaluation of Staining Intensity. The intensity of staining of PECAM-1 on the vascular endothelium was analyzed with an image processing system (Zeiss SEM-IPS; Carl Zeiss, Inc., Thornwood, NY) established in Dr. Paul Knepper's laboratory at Children's Memorial Hospital (Chicago, IL). The sampling window was 0.015 mm^2 and the resolution limit was 0.24 μm. All measurements were made with a planapochromatic 40X/1.0 oil immersion objective under a light microscope (Carl Zeiss, Inc.). They were made as the percentage of transmission with the use of a scanning spectrophotometer (Carl Zeiss, Inc.) with the wavelength set at 500 ± 10 nm. The proper wavelength was determined by a system (Zonax; Carl Zeiss, Inc.). Briefly, spectral scans were performed using a computer-controlled scanning monochromator (Carl Zeiss, Inc.) that scans a spectrum between 400 and 700 nm in 10-nm increments. The spectral data were then corrected for microscope lighting (tungsten lamp), and the wavelength was selected at a range slightly off the maximal adsorption so the dark end of the measurement range would not be saturated. A zero transmission value was set with a black background. A 100% transmission value was measured as the average value of an empty field. Four corneas from each treatment group were excised, and frozen sections were stained together for PECAM-1 as described above. The staining intensity of the corneal

[1] *Abbreviations used in this paper:* H&E, hematoxylin and eosin; HUVEC, human umbilical vein endothelial cells; ICAM, intercellular adhesion molecule; PECAM, platelet endothelial cell adhesion molecule.

blood vessels in each section was measured in a masked fashion. The data were recorded as the average OD per vessel. Using neutral density filters, the Zonax system was found to provide linear readings ($R^2 = 0.9989$) over a scale of 0.1 to 3.0 OD units, which exceeded the range of OD readings for our histologic samples. The image analysis provided an objective evaluation of staining intensity, was in good general agreement with scores based on visual examination, but was able to discriminate differences in staining intensity that would be difficult to discern by microscopic examination alone.

PMN Isolation. PMN were isolated from the peripheral blood by centrifugation on a Percoll gradient using a slight modification of a previously described technique (18). Briefly, blood was collected from the axillary plexus into tubes containing EDTA, diluted with an equal volume of 2× HBSS, and incubated for 15 min at room temperature. The cells were layered over 80% 1.5× hypertonic Percoll (Cell/Flex-1124; Atlanta Biologicals, Inc., Norcross, GA) and centrifuged at 1200 *g* for 30 min at 20°C. Cells from the Percoll–medium interface were washed with 1× HBSS, and residual RBC were lysed with Tris-NH_4Cl. A thioglycolate-induced peritoneal exudate was used as a source of recently extravasated PMN. Mice received an intraperitoneal injection of 1 ml of thioglycolate. 3 h later, the peritoneal exudate was removed, washed once in RPMI 1640 medium supplemented with 5% FCS, and then incubated on a plastic surface for 1 h at 37°C in the same medium. The nonadherent cells were removed and shown to be >98% PMN based on nuclear morphology.

Flow Cytometric Analysis of Adhesion Molecule Expression on PMN. Levels of PECAM-1 or MHC class I on PMN obtained from the peripheral blood or a thioglycolate-induced peritoneal exudate was assessed by flow cytometry (Coulter EPICS V; Coulter Corp., Hialeah, FL). The enriched PMN ($0.5–1 \times 10^6$) were added to the U-bottom wells of a 96-well plate and treated with Fc Block (0.5 μg/10^6 cells of anti-CD32/CD16; PharMingen, San Diego, CA) for 10 min on ice. The cells were then treated with biotinylated mAb to PECAM-1 (2 μg/10^6 cells) or with a similar concentration of a biotinylated rat mAb of irrelevant specificity and incubated on ice for 30 min. The cells were washed and exposed to 100 μl of 5 μg/ml strepavidin-PE (PharMingen) for 30 min. Alternatively, after treatment with Fc Block, the cells were exposed to an unconjugated rat mAb specific for mouse MHC class I, followed by FITC-conjugated goat anti–rat Ig. All cells were then washed and resuspended in PBS containing 5% FCS, 0.1% NaN3, and 130 μg/ml of propidium iodide.

The flow cytometric analysis of PECAM-1 and MHC class I expression was restricted to live PMN based on forward angle and 90° light scatter, and exclusion of propidium iodide–stained cells. A sample of the gated cells was collected, and an H&E-stained cytospin preparation was found to be >98% PMN based on morphology.

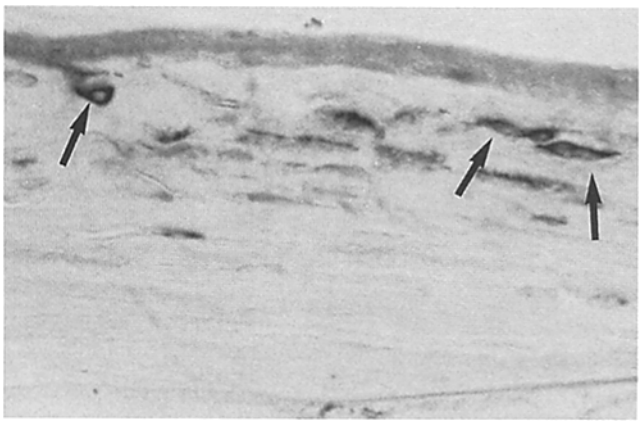

Figure 1. IFN-γ producing cells in HSV-1–infected corneas. Frozen sections were prepared from eyes with 2+ corneal inflammation at day 12–14 after infection. IFN-γ–expressing cells in the cornea (*arrows*) were detected by ABC immunoperoxidase staining. ×132.

Results

Role of IFN-γ in the Maintenance and Progression of Corneal Inflammation. Previous studies involving in vivo neutralization of IFN-γ before HSV-1 corneal infection demonstrated a requirement for IFN-γ in the initiation of the inflammatory response (4). However, the involvement of IFN-γ in the progression of corneal inflammation was not assessed. To clarify this issue, we performed experiments in which in vivo neutralization of IFN-γ was initiated when mice reached the 1+, 2+, or 3+ level of corneal inflammation. In our model, 50–60% of infected corneas developed 1+ to 2+ inflammation from day 10 to 14 after infection, and reached 3+ or even corneal perforation (4+) by day 17–20 after infection. Numerous IFN-γ–producing cells were detected in the corneas at all stages of inflammation, as illustrated in Fig. 1.

Neutralization was accomplished by an intraperitoneal injection of 0.5 mg of IFN-γ–neutralizing mAb, followed by a second injection of 0.5 mg of the same mAb 7 d later. Preliminary experiments and previously published results (2, 4) established that corneal disease, as evaluated clinically or histologically, developed in an identical manner when control mice received an intraperitoneal injection of rat mAb of irrelevant specificity (anti-HLA-DR) or PBS (data not shown). Therefore, in these experiments, control mice received intraperitoneal injections of PBS. Corneal disease was monitored by daily slit-lamp examination until the disease pattern stabilized. The PBS-treated control mice showed progression of corneal inflammation that is typical for our model. When mice were treated with PBS at the 2+ stage of corneal inflammation (10–14 d after infection), all progressed to more severe disease (Fig. 2 *A*), and 50% of the infected corneas of PBS-treated mice became so severely inflamed that the cornea perforated (4+ disease). Similar treatment with anti–IFN-γ resulted in a rapid reversal of corneal inflammation. As early as 2 d after anti–IFN-γ treatment, inflammation in some corneas was completely resolved (Fig. 2 *B*). The disease pattern stabilized 12 d after the initial treatment, when 55% of the corneas of mAb-treated mice improved to normal, 36% remained at a nonprogressive 2+ stage, only 9% progressed to the 3+ stage of inflammation, and none of the corneas of treated mice perforated.

Initiation of anti–IFN-γ mAb treatment when mice were at the 1+ stage of corneal inflammation resulted in complete resolution of inflammation in all corneas within 8 d of the initial treatment (not shown). Treatment with anti–

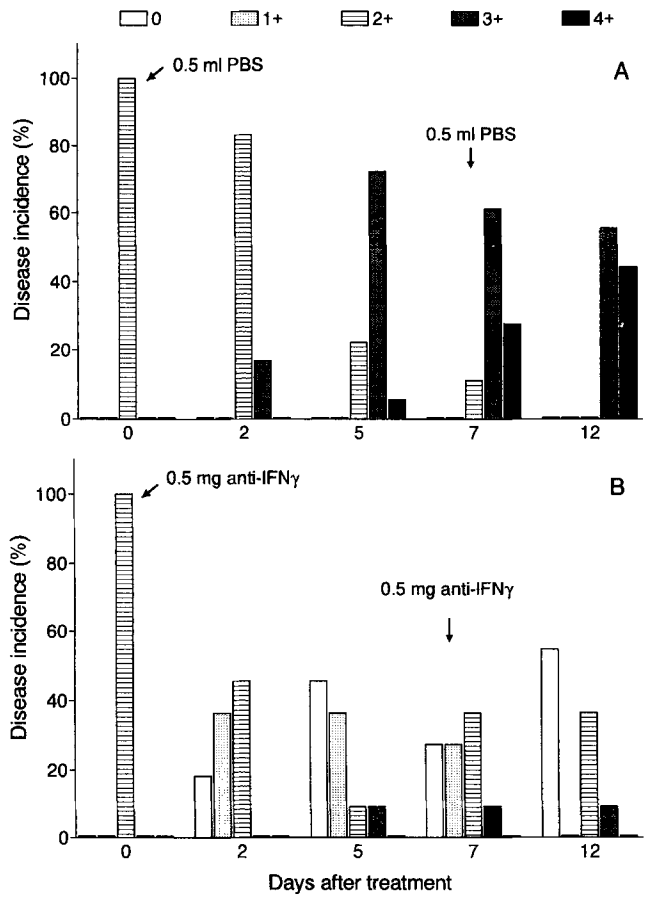

Figure 2. IFN-γ is required for the progression of HSV-1–induced corneal inflammation. Groups of 20–22 mice at the 2+ stage of corneal inflammation received an intraperitoneal injection of 0.5 ml of PBS (*A*) or 0.5 mg of IFN-γ–neutralizing mAb (*B*), and corneal inflammation was monitored by slit-lamp examination. A second identical treatment was administered 7 d later. Data are recorded as the percentage of mice exhibiting different degrees of inflammation. Disease progression was significantly greater ($P < 0.0001$) in the PBS-treated controls than in the anti–IFN-γ–treated mice as assessed by Fisher's exact test.

IFN-γ mAb that was initiated at the 3+ stage of corneal inflammation did not result in an apparent improvement in the clinical condition of the corneas. It is noteworthy, however, that even in the latter group, none of the mice progressed to corneal perforation, and histologically the inflammation appeared to be resolving (not shown). Failure of mAb treatment to improve the clinical condition of 3+ corneas was probably due to preexisting, irreversible structural damage to the cornea at the time of treatment. These results demonstrate that IFN-γ is required during all stages of the progression of the inflammatory response in HSV-1–infected corneas.

Role of IFN-γ in Leukocyte Extravasation. To investigate the mechanisms by which IFN-γ regulates the progression of inflammation, we compared histologic changes in corneas with 2+ inflammation after intraperitoneal injection of anti–IFN-γ mAb with those in control (anti–HLA-DR5) mAb–treated mice. The cornea is normally avascular, but corneal inflammation is accompanied by gradual neovascularization. During the early stages of inflammation, the leukocytes extravasate from blood vessels in the peripheral cornea, and then migrate to the central cornea. At the 2+ stage of HSV-1–induced corneal inflammation, blood vessels had begun to invade the corneal stroma, and a dense infiltrate consisting of PMN (Fig. 3 *A*) and $CD3^+$ T cells (Fig. 3 *B*) was observed in the perivascular space. Within 48 h after anti–IFN-γ treatment, a marked reduction of PMN infiltration into the perivascular space was observed (Fig. 3 *C*), whereas the density of $CD3^+$ T cells was not noticeably affected (Fig. 3 *D*). As a specificity control, mice received similar treatment with an IL-2–neutralizing mAb. The anti–IL-2 treatment did not influence the infiltration of PMN (Fig. 3 *E*) or $CD3^+$ T cells (Fig. 3 *F*) into the perivascular space. Thus, IFN-γ mediates inflammation in HSV-1–infected corneas, at least in part by regulating PMN extravasation from blood vessels in the peripheral cornea.

Modulation of Adhesion Molecule Expression by IFN-γ. ICAM-1 was not detectable by immunohistochemical staining on the vascular endothelium of normal mouse corneas, but its expression was markedly upregulated on the vascular endothelium of infected corneas at the 2+ stage of inflammation (Fig. 4 *A*). Because ICAM-1 is essential for PMN extravasation in some models (19–22), and its expression on vascular endothelial cells can be induced by IFN-γ (10–12, 14), we hypothesized that in vivo neutralization of IFN-γ might have blocked PMN extravasation into HSV-1–infected corneas by reducing ICAM-1 expression in the lumen of corneal vessels. However, ICAM-1 expression on the corneal vascular endothelium was not noticeably reduced up to 48 h after anti–IFN-γ treatment (Fig. 4 *B*), a period when PMN infiltration into the perivascular space was blocked. Anti–IFN-γ treatment also failed to alter the expression of Mac-1 and LFA-1, the leukocyte counterreceptors for ICAM-1 on the small number of leukocytes that did infiltrate the corneas of anti–IFN-γ–treated mice (data not shown). The failure of anti–IFN-γ treatment to alter the expression of these adhesion molecules suggests either that IFN-γ is not necessary for regulating their expression in our model or that a slow turnover rate of these molecules on vascular endothelial cells and leukocytes precluded detection in the time frame of our experiments. In either case, it would appear that anti–IFN-γ treatment does not block PMN extravasation through modulation of ICAM-1 expression on corneal vascular endothelium in our model.

Recent studies have established a role for PECAM-1 in PMN extravasation in vitro and in vivo (23–25). PECAM-1 is expressed constitutively at low levels on peripheral blood vessels in normal mouse corneas (not shown), and its expression was strongly upregulated in infected corneas with 2+ inflammation (Fig. 5, *A* and *B*). Within 24 h after anti–IFN-γ treatment of mice with 2+ corneal inflammation, PECAM-1 expression on corneal vascular endothelium was noticeably reduced (not shown). By 48 h after treatment, PECAM-1 expression was reduced to a level that is consti-

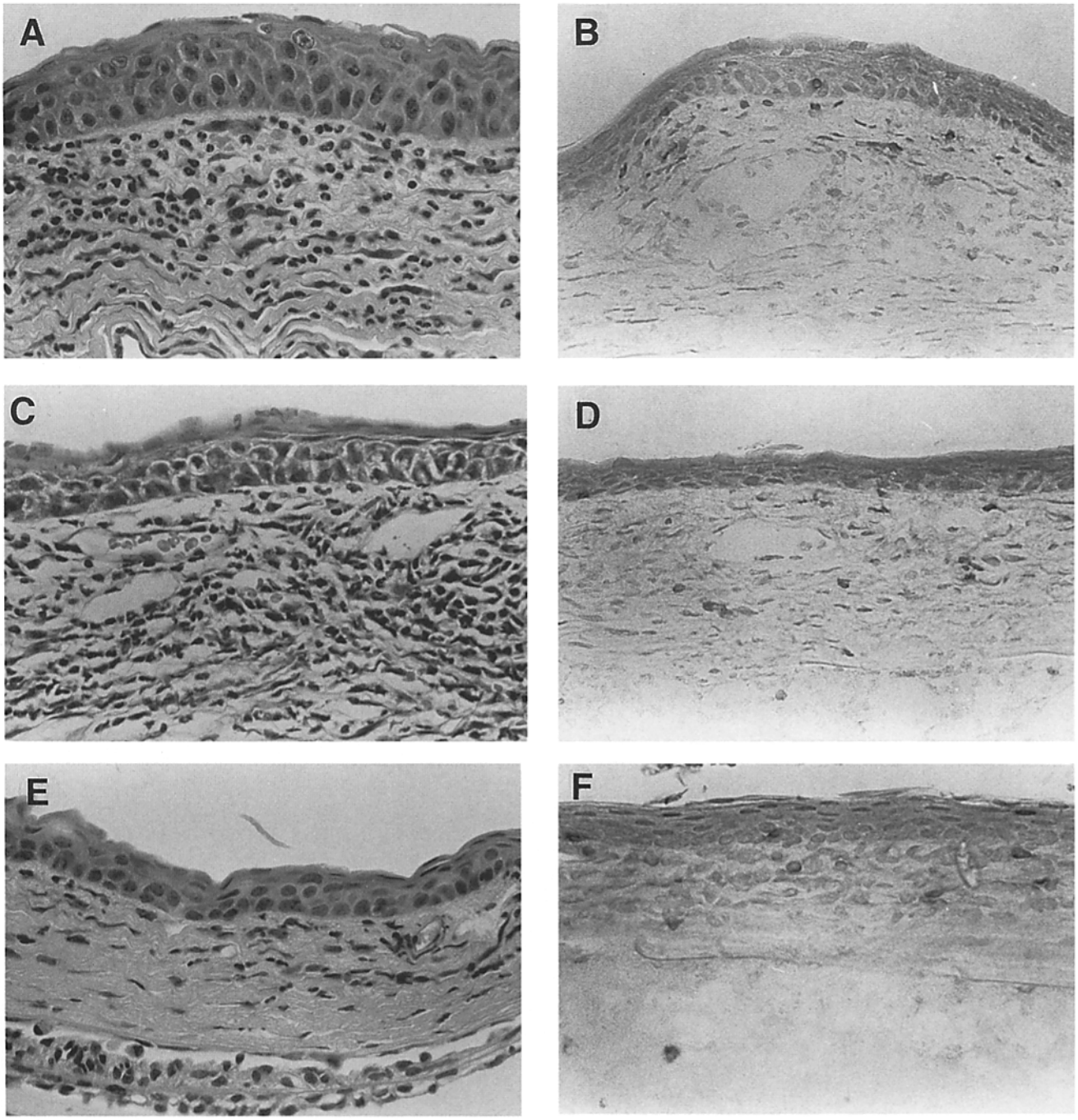

Figure 3. Representative photomicrographs illustrating the effect of IFN-γ neutralization on leukocyte infiltration into HSV-1–infected corneas. HSV-1–infected mice exhibiting the 2+ level of corneal inflammation received an intraperitoneal injection of PBS, an IFN-γ–neutralizing rat mAb, or an IL-2–neutralizing rat mAb, and 48 h later corneas were examined histologically. H&E stained paraffin sections of corneas from PBS-treated mice (*A*) and anti–IL-2–treated mice (*C*) showed a heavy PMN infiltration into the perivascular space, which was markedly reduced in anti–IFN-γ–treated mice (*E*). In contrast, immunohistochemical staining revealed similar numbers of $CD3^+$ T cells in corneas from PBS-treated (*B*), anti–IL-2–treated (*D*), and anti–IFN-γ–treated mice (*F*). ×132.

tutively expressed in normal corneas (Fig. 5, *C* and *D*). The reduction of PECAM-1 expression correlated temporally with the inhibition of PMN extravasation in the corneas.

To quantitatively assess the effect of IFN-γ neutralization on PECAM-1 expression on the corneal vascular endothelium, HSV-1–infected mice with 2+ corneal inflammation received an intraperitoneal injection of anti–IFN-γ mAb or a control rat mAb (anti–HLA-DR5). 2 d later, corneas from the two treatment groups, or from normal (noninfected mice) were removed, and frozen sections were stained simultaneously and under identical conditions for PECAM-1. In masked studies, the level of PECAM-1

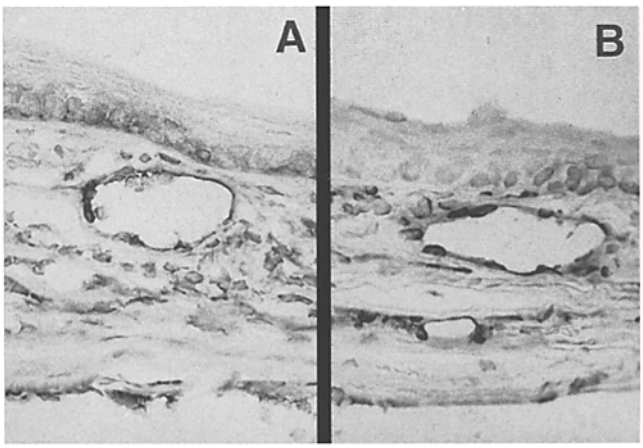

Figure 4. Representative photomicrographs illustrating the effect of IFN-γ neutralization on vascular endothelial expression of ICAM-1 in HSV-1–infected corneas. HSV-1–infected mice exhibiting the 2+ level of corneal inflammation received an intraperitoneal injection of PBS (*A*) or anti–IFN-γ (*B*), and 48 h later corneas were examined for ICAM-1 expression by immunohistochemistry. Treatment did not markedly influence ICAM-1 expression. ×100.

expression on vascular endothelium was assessed by image analysis as described in Materials and Methods. The data obtained from scans of 40 sections of vessels in infected corneas of anti–IFN-γ–treated mice, 42 vessels in infected corneas of control mAb–treated mice, and 17 vessels in normal corneas are recorded in Fig. 6 as the average staining intensity (OD) of each vessel. By 48 h after anti–IFN-γ treatment, PECAM-1 expression on the vascular endothelium was significantly reduced ($P < 0.001$) when compared with PECAM-1 expression on vessels of PBS-treated controls. The level of PECAM-1 expression on vascular en-

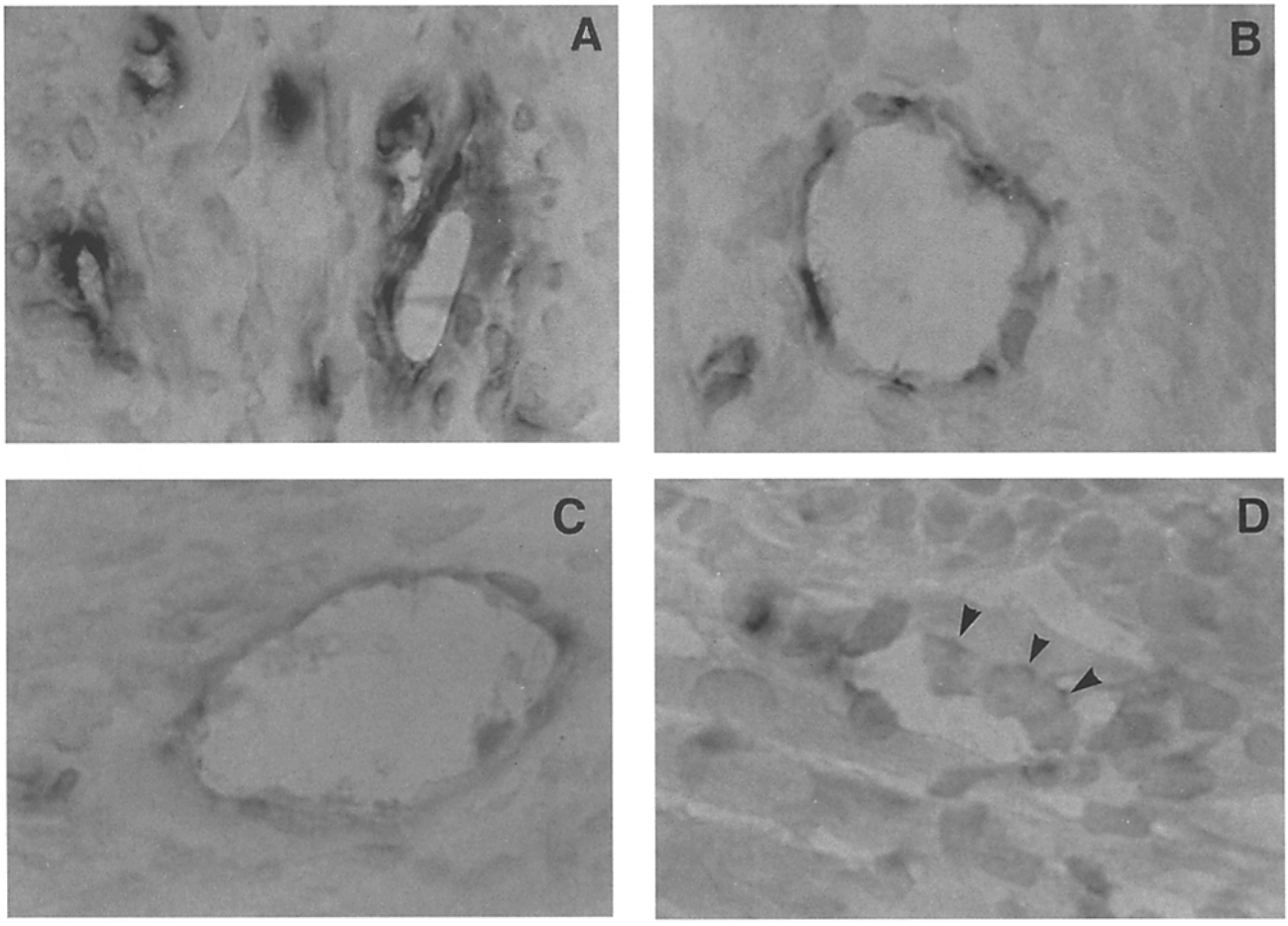

Figure 5. Representative photomicrographs illustrating the effect of IFN-γ neutralization on PECAM-1 expression on vascular endothelium of HSV-1–infected corneas. HSV-1–infected mice exhibiting the 2+ level of corneal inflammation received an intraperitoneal injection of control mAb (anti–HLA-DR5) or anti–IFN-γ, and PECAM-1 expression was evaluated by immunohistochemistry. PECAM-1 expression remained high 48 h after control mAb treatment (*A* and *B*) but was markedly reduced 48 h after anti–IFN-γ treatment (*C* and *D*). Depicted are vessels with the highest (*A*) and average (*B*) PECAM-1 expression in controls, and the average (*C*) and lowest (*D*) PECAM-1 expression in anti–IFN-γ–treated mice. The average staining intensity of these vessels, as assessed by image analysis, was 0.44 (*A*), 0.25 (*B*), 0.12 (*C*), and 0.02 (*D*). These fields were chosen to represent the range of staining intensities shown in Fig. 6. Note the accumulation of PMN (*arrowheads*) in the lumen of vessels with low PECAM-1 expression. ×330.

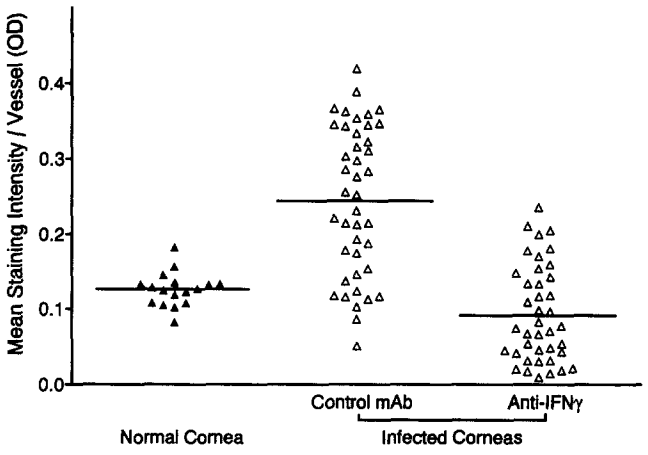

Figure 6. IFN-γ neutralization reduces PECAM-1 expression on the vascular endothelium of HSV-1–infected corneas (*open symbols*) to approximately that of normal corneas (*solid symbols*). HSV-1–infected mice exhibiting the 2+ level of corneal inflammation received an intraperitoneal injection of control mAb (anti–HLA-DR5) or anti–IFN-γ, and infected and normal corneas were excised 48 h later. Frozen sections of corneas from four mice per group were examined for PECAM-1 expression by ABC immunoperoxidase staining. The level of PECAM-1 expression was assessed in a masked fashion by image analysis as described in Materials and Methods, and recorded as the mean staining intensity (OD) per corneal vessel. The mean level of PECAM-1 expression in each group is indicated by a solid line. The data were analyzed by a one-way analysis of variance followed by Tukey's posttest. PECAM-1 expression was significantly elevated in the control mAb group ($P < 0.001$) but not in the anti–IFN-γ–treated group ($P > 0.05$) when compared with normal corneas. PECAM-1 expression was significantly lower ($P < 0.001$) in anti–IFN-γ–treated mice than in control mAb–treated mice.

dothelium of infected corneas 48 h after anti–IFN-γ treatment was not significantly different ($P > 0.05$) from that constitutively expressed on vascular endothelium of normal corneas. The magnitude of the difference in staining intensity in treated and control corneas, as assessed by image analysis, can be visualized in Fig. 5. The staining intensity of vessels in Fig. 5, *A–D*, were 0.48, 0.25, 0.12, and 0.02, respectively. This result is consistent with the hypothesis that IFN-γ is required for maintaining a high level of PECAM-1 expression on the vascular endothelium of HSV-1–infected corneas, and that a high level of PECAM-1 expression is required for PMN extravasation.

We noted that the level of PECAM-1 expression was quite consistent in vessels of a given cornea, and very consistent on the same vessel in serial sections. It was possible, therefore, to evaluate PMN extravasation in serial sections adjacent to those that exhibited high (0.2–0.4 OD) and low (0–0.2 OD) expression of PECAM-1 on corneal vessels. Sections were simultaneously stained for PECAM-1 and PMN using a two-color immunofluorescent stain. As illustrated in Fig. 7, vessels that expressed a high concentration of PECAM-1 showed a heavy density of PMN in the perivascular space. In contrast, those vessels exhibiting barely detectable PECAM-1 showed no evidence of PMN extravasation.

The photomicrographs in Figs. 5 *D* and 7 illustrate two additional points that are of interest. First, we note that PMN tend to accumulate in the lumen of vessels that exhibit low levels of PECAM-1 expression. This is consistent with our observation that ICAM-1 expression remains high in these vessels. Taken in the context of the current paradigm of the adhesion cascade that controls PMN extravasation, this observation would suggest that integrin-mediated tethering of the PMN to the vascular endothelium is not altered by IFN-γ neutralization, but PECAM-1–mediated transendothelial migration is blocked.

PMN in the peripheral blood have been shown to express low but detectable levels of PECAM-1 (26). We noted a low level of PECAM-1 staining on PMN that were trapped in the lumen of vessels of anti–IFN-γ–treated mice (Figs. 5 *D* and 7 *E*). Interestingly, PMN that extravasated into the cornea did not express detectable PECAM-1 (Figs. 5 *A* and 7 *B*). This suggested that PECAM-1 expression on PMN is dramatically reduced after extravasation. However, to clearly establish this point required flow cytometric analysis. Because it is difficult to extract sufficient PMN from the cornea for flow cytometric analysis, we chose as an alternative to compare PECAM-1 expression on PMN obtained from the peripheral blood of mice with PECAM-1 expression on PMN obtained from a thyoglycolate-induced peritoneal exudate. Thus, PMN obtained from the peripheral blood or peritoneal exudate were stained with biotin-conjugated anti–PECAM-1 or an isotype-matched, biotin-conjugated mAb of irrelevant specificity, followed by PE-conjugated avidin. As illustrated in Fig. 8, PECAM-1 expression was markedly reduced on PMN that had recently extravasated into the peritoneal cavity (mean fluorescence intensity [channel] = 39.9, mean channel difference [compared with control mAb] = 1.3) when compared with PMN from the peripheral blood (mean fluorescence intensity = 99.6, mean channel difference = 54.4). A similar analysis of MHC class I expression revealed elevated expression on the peritoneal exudate PMN (mean fluorescence intensity = 131.5, mean channel difference = 68.1) when compared with those from the peripheral blood (mean fluorescence intensity = 110.5, mean channel difference = 30.3). The peritoneal exudate PMN lacked detectable PECAM-1 expression whether or not they were depleted of macrophages (data not shown), ruling out the possibility that PECAM-1 was selectively lost from peritoneal exudate PMN during the 1-h incubation on plastic to remove macrophages. Thus, PECAM-1 appears to be lost from PMN during extravasation in a manner analogous to L-selectin, whereas MHC class I expression is elevated during this process.

PECAM-1 is a recently described member of the adhesion molecule family, and the regulation of its expression is not yet well documented. To confirm our finding that IFN-γ regulates PECAM-1 but not ICAM-1 expression on vascular endothelium in vivo, 100 U of mouse rIFN-γ was injected into normal mouse corneas, and the corneas were monitored for PECAM-1 and ICAM-1 expression by immunohistochemistry and image analysis. As shown in Fig. 9, PECAM-1 was constitutively expressed at a low

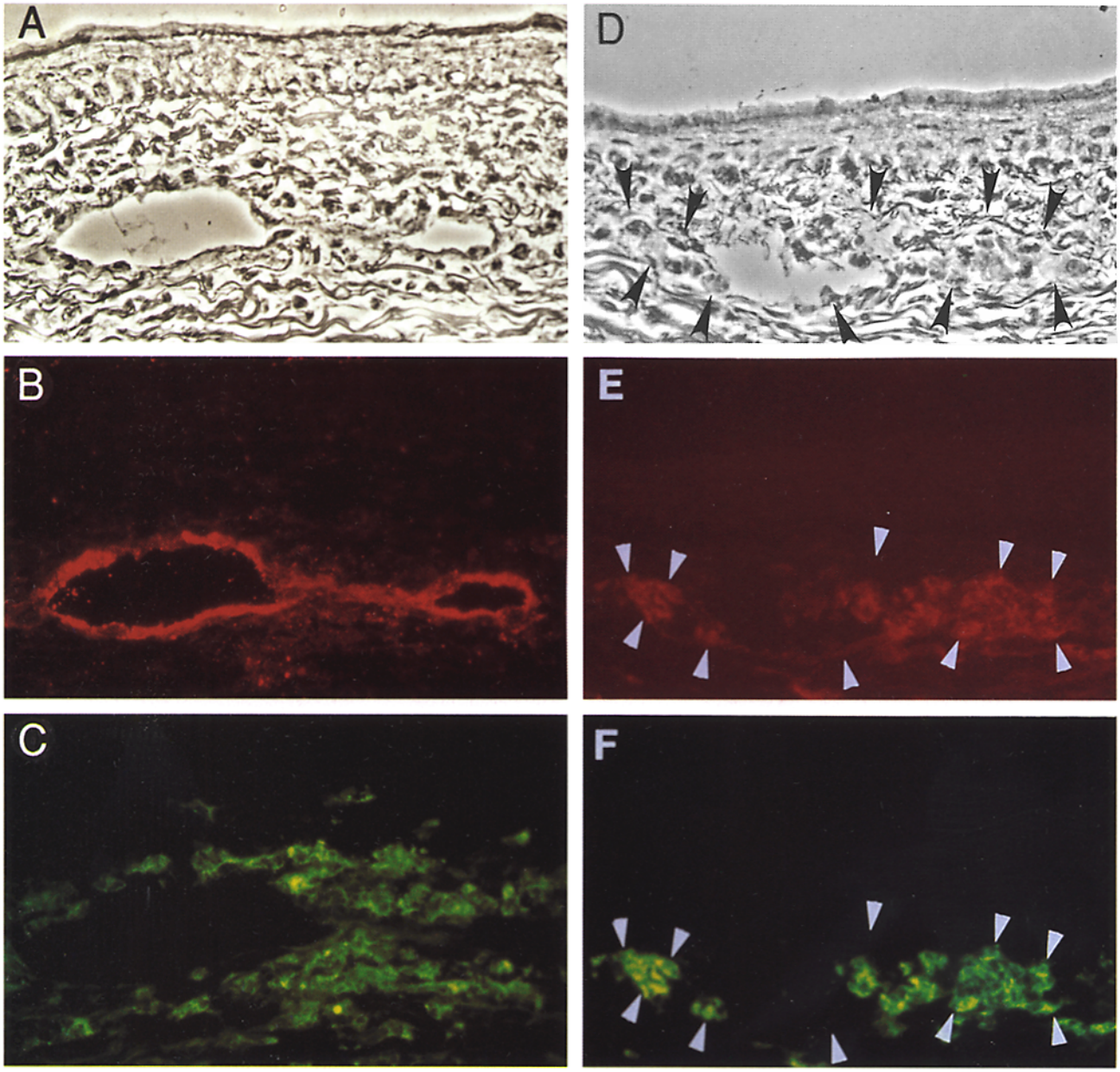

Figure 7. Relationship between PECAM-1 expression on corneal vessels and PMN extravasation. HSV-1–infected mice exhibiting the 2+ level of corneal inflammation received an intraperitoneal injection of anti–IFN-γ. After 48 h, two-color immunofluorescence staining of frozen sections of the corneas was used to simultaneously identify PECAM-1 expression on vascular endothelium (phycoerytherin, *red*) and PMN (FITC, *green*). Phase contrast shows the location of corneal blood vessels (*A* and *D*). The accumulation of PMN in the lumen of vessels of anti–IFN-γ–treated corneas tends to obscure the vessel walls (*arrowheads*). Corneas with high PECAM-1 expression on the vascular endothelium (*B*) exhibited large numbers of PMN in the perivascular space (*C*). In contrast, corneas expressing barely detectable levels of PECAM-1 on the vascular endothelium (*E*) showed very few PMN in the perivascular space (*F*). Note the accumulation of PMN in the lumen of vessels with reduced PECAM-1 expression (*F*). ×132.

level on normal corneal vascular endothelium, and that level of expression was not significantly altered by intracorneal injection of PBS. However, PECAM-1 expression was strongly upregulated 3 h after injection of rIFN-γ. In contrast, ICAM-1 was not detectable on normal vascular endothelial cells, and its expression was not induced at any time after injection of rIFN-γ (data not shown). This result lends further support to the notion that PECAM-1 but not ICAM-1 expression is regulated by IFN-γ in the inflamed cornea after HSV-1 infection. Although the level of PECAM-1 expression induced by rIFN-γ appears to be as high as that observed in the inflamed corneas, no infiltrating PMN were seen in the rIFN-γ–injected corneas at the time points examined. This suggests PECAM-1 expression

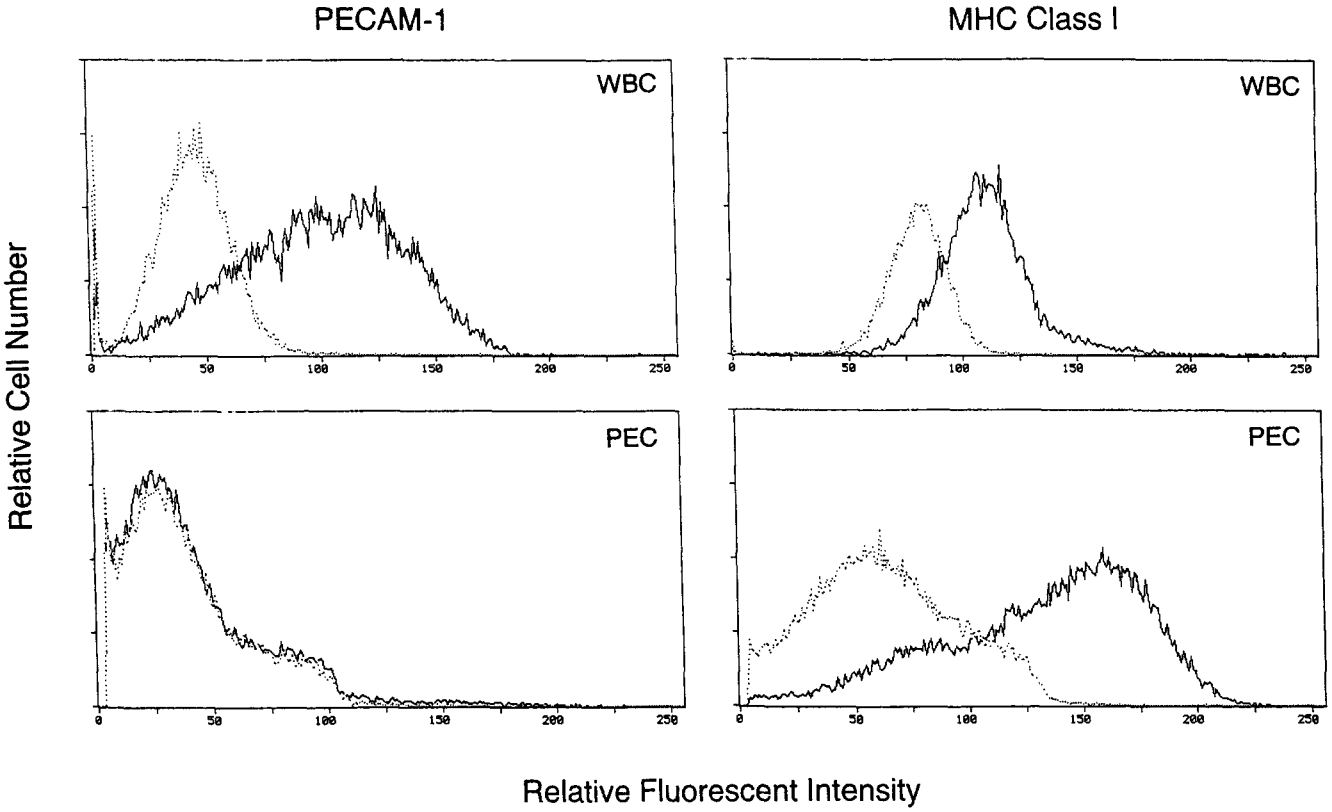

Figure 8. PECAM-1 and MHC class I expression profile of mouse PMN freshly isolated from circulating white blood cells (*WBC*) or of PMN isolated from peritoneal exudate cells (*PEC*). Cells were stained with biotinylated rat mAb to PECAM-1 or with a biotinylated rat mAb of irrelevant specificity followed by PE-conjugated streptavidin; or were stained with rat mAb to a nonpolymorphic region of mouse MHC class I followed by FITC-conjugated anti–rat Ig. The cells were analyzed on a flow cytometer as described in Materials and Methods. PMN that extravasated into the peritoneal cavity resembled those that extravasated into the cornea in that they expressed lower levels of PECAM-1 but elevated levels of MHC class I when compared with PMN in the peripheral blood.

alone is not sufficient for PMN extravasation, which is likely to require orchestrated expression of several adhesion molecules.

Discussion

Despite the availability of effective antiherpetic drugs, HSV-1 corneal infections continue to be a major contributor to visual morbidity. The ability of the virus to establish a latent infection in the sensory neurons makes eradication of the virus from the infected individual impossible at the present time. For this reason, we believe our best current hope for improved ophthalmic treatment lies in a better understanding of the pathological processes that contribute to the corneal destruction associated with HSV infection. Toward this end, we have established a mouse model of the disease. Using the mouse model, we and others have demonstrated that corneal destruction is not a direct effect of the virus, but rather is the consequence of a T lymphocyte response to HSV antigens (2–4, 27–36). Paradoxically, a T lymphocyte response also contributes to prevention of virus spread to the periocular skin and to the brain (29, 34). It becomes imperative, therefore, to understand the immunologic mechanisms that may uniquely contribute to the proinflammatory environment within the infected cornea and that may be subject to local regulation.

Previous studies from our laboratory have established that the Th1 cytokines IL-2 and IFN-γ are requisite mediators of the inflammatory response to HSV-1 in the mouse cornea (4). In those studies, corneal inflammation was prevented by treating mice systemically with mAb to IL-2 or IFN-γ. However, a more clinically relevant question may be whether these mAb can treat existing inflammation. In addition, preventing disease does not offer an opportunity to identify mechanisms by which these molecules participate in the inflammatory process. In this report, we demonstrate that mAb to IFN-γ can be effective in ameliorating established HSV-1–induced corneal inflammation. Treatment with anti–IFN-γ mAb had a palliative effect when initiated at all stages of inflammation, suggesting that IFN-γ is required both for initiation and for maintenance or progression of the inflammatory process. These findings suggest that appropriate manipulation of the proinflammatory functions of IFN-γ might provide an effective means of intervening in the inflammatory process. We were thus encouraged to pursue studies designed to define the mechanisms by which IFN-γ regulates inflammation in HSV-1–infected mouse corneas.

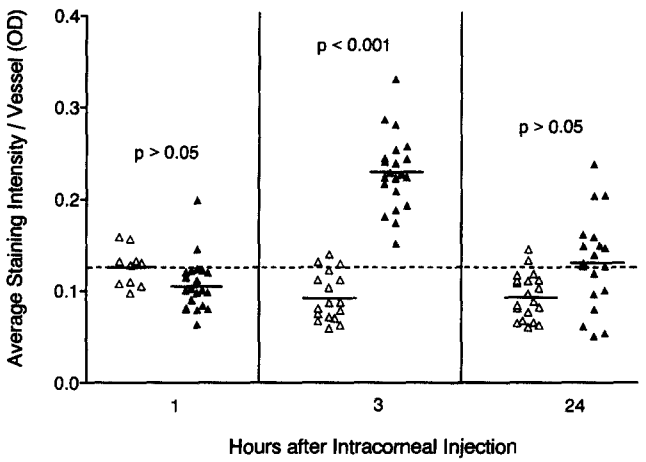

Figure 9. Induction of PECAM-1 expression on corneal vascular endothelium after intrastromal injection of rIFN-γ into normal mouse corneas. Mouse rIFN-γ (100 U in 0.5 μl of PBS [▲]) or 0.5 μl of PBS alone (△) was injected into normal mouse corneas. At the indicated time after injection, frozen sections of corneas from four mice per group were examined for PECAM-1 expression by ABC immunoperoxidase staining. The level of PECAM-1 expression was assessed in a masked fashion by image analysis as described in Materials and Methods and recorded as the mean staining intensity (OD) per corneal vessel. The mean level of PECAM-1 expression on vessels in injected corneas is indicated by a solid line; the mean level of PECAM-1 expression on vessels of normal corneas is indicated by the dotted line. Data from all three groups were analyzed by a one-way analysis of variance followed by Tukey's multiple comparison test. The *P* values are for a comparison of the PECAM-1 expression in PBS and rIFN-γ–injected corneas. PECAM-1 expression in PBS-treated corneas did not differ significantly from that in normal corneas at any time ($P > 0.05$). PECAM-1 expression in the rIFN-γ–injected corneas was significantly ($P < 0.001$) higher than that in normal corneas at 3 h but was not significantly different ($P > 0.05$) at 1 or 24 h.

Our histologic studies have provided some important clues to how IFN-γ regulates inflammation in the cornea. Within 48 h after treatment with mAb to IFN-γ, a marked reduction in the number of PMN in the perivascular space of the peripheral cornea was noted. The specificity of this effect was emphasized by the fact that similar treatment with mAb specific for IL-2, while also reducing inflammation in the HSV-1–infected cornea (Tang, Q., W. Chen, and R.L. Hendricks, manuscript submitted for publication), did not block PMN extravasation (Fig. 3). These observations demonstrated a role for IFN-γ in regulating PMN extravasation into infected corneas. In contrast, the continued presence of T lymphocytes in the perivascular space of the cornea after treatment with mAb to IFN-γ suggests either that IFN-γ does not regulate T lymphocyte extravasation or that the T lymphocytes that were present in the perivascular space of treated mice had extravasated before treatment but failed to migrate out of the perivascular region.

Previous investigations established that IFN-γ treatment differentially increases adhesion of T cells, but not PMN, to cultured endothelial cells (37). In addition, intradermal injection of IFN-γ induces infiltration of T cells and monocytes, but not PMN (38, 39). Taken together with our current findings, these results suggest that (*a*) IFN-γ is necessary, but perhaps not sufficient, for PMN extravasation; and (*b*) IFN-γ is sufficient, but may not be necessary, for T cell extravasation. In the latter case, other inflammatory cytokines that are present in the milieu of the inflamed cornea may supplant the role of IFN-γ in T lymphocyte extravasation.

Treatment with anti–IFN-γ could regulate PMN extravasation by altering the pattern of adhesion molecule expression on the vascular endothelium. ICAM-1 and PECAM-1 are Ig superfamily adhesion molecules that have been shown to participate in the interaction of PMN with the vascular endothelium. ICAM-1 expression on the vascular endothelium is regulated by a variety of proinflammatory mediators including IFN-γ (10, 11, 40–43). The importance of ICAM-1 for PMN extravasation at inflammatory sites appears to vary when tested in different models of acute inflammation (19–22, 44–47). Although we observed increased expression of ICAM-1 on the corneal vascular endothelium after HSV-1 infection, its expression was not altered by anti–IFN-γ treatment during the period that inhibition of PMN extravasation was noted. Our results do not imply a lack of ICAM-1 involvement in PMN extravasation in this model, but only that inhibition of PMN extravasation into HSV-1–infected corneas of anti–IFN-γ treated mice was not effected through modulation of ICAM-1 expression. This result might be expected because several cytokines, including TNF-α and IL-1, that are capable of inducing ICAM-1 expression on vascular endothelium have been shown to be produced in HSV-1–infected corneas (3, 48).

PECAM-1 is constitutively expressed on vascular endothelium and concentrated in the endothelial junctions (23). IFN-γ regulation of PECAM-1 expression on human umbilical vein endothelial cells (HUVEC) has been studied in vitro. One study (49) revealed a moderate increase in PECAM-1 expression on HUVEC after exposure to IFN-γ. However, a more recent study (50) demonstrated that IFN-γ did not change PECAM-1 transcription or total surface expression on HUVEC, but did induce a redistribution of PECAM-1 away from intracellular junctions. The reason for the difference in PECAM-1 regulation in the two studies is not clear, but may relate to the condition of the HUVEC at the time of assay. For instance, low constitutive expression of PECAM-1 on HUVEC may be upregulated by IFN-γ, whereas high constitutive expression may be unaffected.

To our knowledge, our study is the first to examine IFN-γ regulation of PECAM-1 expression on vascular endothelium in vivo. We observed a rather dramatic upregulation of PECAM-1 expression when IFN-γ was injected into a normal cornea, and an equally dramatic downregulation when IFN-γ was neutralized in an inflamed cornea. The kinetics of the two reactions was quite similar. PECAM-1 expression in the cornea was significantly increased 3 h after injection of IFN-γ, and then returned to baseline levels by 24 h. Similarly, reduction of PECAM-1 expression in inflamed corneas became apparent 24 h after treatment with anti–IFN-γ mAb, with the maximal effect seen at 48 h. The seemingly more dramatic regulatory ef-

fect of IFN-γ on PECAM-1 expression in vivo may reflect among other things (*i*) functional changes in endothelial cells during in vitro culture, (*ii*) functional differences associated with the tissue of origin (i.e., normally avascular cornea versus the highly vascularized umbilical cord), or (*iii*) species differences. PECAM-1 contributes to the junctional integrity of the vascular endothelium (51) and may have a role in neovascularization (52). It is interesting to speculate that the cornea may normally maintain its avascularity and discourage inflammatory responses by inhibiting PECAM-1 expression on the endothelium of peripheral vessels. IFN-γ may overcome this inhibitory effect, and thus dramatically increase PECAM-1 expression. The increased PECAM-1 expression may facilitate both neovascularization and PMN extravasation into the cornea.

We demonstrate a good correlation between the degree of PECAM-1 expression on corneal vascular endothelium and the number of PMN in the perivascular space. Moreover, PMN were consistently seen to accumulate in the lumen of corneal vessels after IFN-γ neutralization. This observation is consistent with the notion that the continued high level of expression of ICAM-1 observed on the vascular endothelium of these mice permits the β2 integrin–mediated firm adhesion of the PMN to the walls of the corneal vessels, whereas their transendothelial migration is blocked. Although correlative, our results strongly suggest that PECAM-1 is an important regulator of PMN extravasation in the chronically inflamed HSV-1–infected cornea. This is consistent with the observation that PECAM-1 plays an important role in PMN extravasation at sites of acute inflammation (23–25).

Evidence suggests that homophilic interaction of PECAM-1 on PMN and vascular endothelium is required for transendothelial migration (23). Our observation that PMN within the blood vessels express readily detectable levels of PECAM-1 is consistent with the proposal put forth by other investigators (23) that a homophilic interaction of PECAM-1 on the PMN and vascular endothelium may permit the PMN to pass through the endothelial junction in a zipper-like fashion. We also observed that PMN that extravasated into the cornea or into the peritoneal cavity lacked detectable PECAM-1. We cannot currently rule out the possibility that the apparent loss of PECAM-1 actually reflects the loss of the particular epitope on PECAM-1 that is recognized by the anti–PECAM-1 mAb used in these studies. However, a more appealing interpretation would be that movement of the PMN through the endothelial junction is facilitated by shedding of PECAM-1 from the surface of the PMN. Such a model would be consistent with the observation of Bogen et al. (26) that CD31 is predominantly distributed on portions of transmigrating lymphocytes that are in contact with or adjacent to areas of contact with endothelial cells. However, there is also published evidence that heterophilic interactions of PECAM-1 may facilitate migration of PMN through the vascular basement membrane (53, 54). Thus, it is not clear at what stage in the extravasation process PECAM-1 is lost from the surface of the PMN.

We believe the cornea is an ideal tissue in which to study immunologically mediated inflammation. Its transparent nature permits in vivo monitoring of many aspects of the inflammatory process such as edema, leukocyte infiltration, and neovascularization. Moreover, its structural simplicity and absence of confounding preexisting immunologic components make it easier to analyze inflammation histologically. In addition, HSV-1 corneal inflammation offers a reproducible model of immunologically mediated inflammation that is of considerable clinical relevance. Therefore, we anticipate that the use of this model will lead both to the elucidation of basic immunologic mechanisms that contribute to chronic inflammation and ultimately to improved treatment of this devastating ophthalmic disease.

This work was supported by National Institutes of Health grants EY05945, EY10359, and core grant EY01792; by an unrestricted research grant from Research to Prevent Blindness, Inc., New York; and by the Lions of Illinois Foundation, Maywood, IL. R.L. Hendricks is a Research to Prevent Blindness Senior Scientific Investigator.

Address correspondence to Dr. Robert. L. Hendricks, Department of Ophthalmology and Visual Sciences, University of Illinois at Chicago, 1855 West Taylor Street, Chicago, IL 60612.

Received for publication 30 January 1996 and in revised form 25 July 1996.

References

1. Hendricks, R.L., P.C. Weber, J.L. Taylor, A. Koumbis, T.M. Tumpey, and J. C. Glorioso. 1991. Endogenously produced interferon alpha protects mice from herpes simplex virus type 1 corneal disease. *J. Gen. Virol.* 72:1601–1610.
2. Hendricks, R.L., and T.M. Tumpey. 1990. Contribution of virus and immune factors to herpes simplex virus type 1 induced corneal pathology. *Invest. Ophthalmol. Vis. Sci.* 31: 1929–1939.
3. Niemialtowski, M.G., and B.T. Rouse. 1992. Predominance of Th1 cells in ocular tissues during herpetic stromal keratitis. *J. Immunol.* 149:3035–3039.
4. Hendricks, R.L., T.M. Tumpey, and A. Finnegan. 1992. IFN-gamma and IL-2 are protective in the skin but pathologic in the corneas of HSV-1-infected mice. *J. Immunol.* 149:3023–3028.
5. Tumpey, T.M., V.M. Elner, S.-H. Chen, J.E. Oakes, and

R.N. Lausch. 1994. Interleukin-10 treatment can suppress stromal keratitis induced by herpes simplex virus type 1. *J. Immunol.* 153:2258–2265.
6. Murray, H.W. 1994. Interferon-gamma and host antimicrobial defense: current and future clinical applications. *Am. J. Med.* 97:459–467.
7. Stout, R.D. 1993. Macrophage activation by T cells: cognate and non-cognate signals. *Curr. Opin. Immunol.* 5:398–403.
8. Farrar, M.A., and R.D. Schreiber. 1993. The molecular cell biology of interferon-gamma and its receptor. *Annu. Rev. Immunol.* 11:571–611.
9. Steinbeck, M.J., and J.A. Roth. 1989. Neutrophil activation by recombinant cytokines. *Rev. Infect. Dis.* 11:549–568.
10. Pober, J.S., M.A. Gimbrone, Jr., L.A. Lapierre, D.L. Mendrick, W. Fiers, R. Rothlein, and T.A. Springer. 1986. Overlapping patterns of activation of human endothelial cells by interleukin 1, tumor necrosis factor, and immune interferon. *J. Immunol.* 137:1893–1896.
11. Doukas, J., and J.S. Pober. 1990. IFN-gamma enhances endothelial activation induced by tumor necrosis factor but not IL-1. *J. Immunol.* 145:1727–1733.
12. Issekutz, A.C., and N. Lopes. 1993. Endotoxin activation of endothelium for polymorphonuclear leukocyte transendothelial migration and modulation by interferon-gamma. *Immunology.* 79:600–607.
13. Ribeiro, R.A., F.Q. Cunha, and S.H. Ferreira. 1990. Recombinant gamma interferon causes neutrophil migration mediated by the release of a macrophage neutrophil chemotactic factor. *Int. J. Exp. Pathol.* 71:717–725.
14. Gerritsen, M.E., M.J. Niedbala, A. Szczepanski, and W.W. Carley. 1993. Cytokine activation of human macro- and microvessel-derived endothelial cells. *Blood Cells.* 19:325–339.
15. Meda, L., S. Gasperini, M. Ceska, and M.A. Cassatella. 1994. Modulation of proinflammatory cytokine release from human polymorphonuclear leukocytes by gamma interferon. *Cell. Immunol.* 157:448–461.
16. Leeuwenberg, J.F.M., E.J.U. Von Asmuth, T.M.A.A. Jeunhomme, and W.A. Buurman. 1990. Interferon-gamma regulates the expression of the adhesion molecule ELAM-1 and IL-6 production by human endothelial cells in vitro. *J. Immunol.* 145:2110–2114.
17. Hendricks, R.L., and J. Sugar. 1984. Lysis of herpes simplex virus-infected targets. II. Nature of the effector cells. *Cell. Immunol.* 83:262–270.
18. Lewinsohn, D.M., R.F. Bargatze, and E.C. Butcher. 1987. Leukocyte-endothelial cell recognition: evidence of a common molecular mechanism shared by neutrophils, lymphocytes, and other leukocytes. *J. Immunol.* 138:4313–4321.
19. Mulligan, M.S., G.P. Wilson, R.F. Todd, III, C.W. Smith, D.C. Anderson, J. Varani, T.B. Issekutz, M. Myasaka, T. Tamatani, J.R. Rusche et al. 1993. Role of β1, β2 integrins and ICAM-1 in lung injury after deposition of IgG and IgA immune complexes. *J. Immunol.* 150:2407–2417.
20. Barton, R.W., R. Rothlein, J. Ksiazek, and C. Kennedy. 1989. The effect of anti-intercellular adhesion molecule-1 on phorbol-ester-induced rabbit lung inflammation. *J. Immunol.* 143:1278–1282.
21. Mulligan, M.S., G.O. Till, C.W. Smith, D.C. Anderson, M. Miyasaka, T. Tamatani, R.F. Todd, III, T.B. Issekutz, and P.A. Ward. 1994. Role of leukocyte adhesion molecules in lung and dermal vacular injury after thermal trauma of skin. *Am. J. Pathol.* 144:1008–1015.
22. Yoshida, N., D.N. Granger, D.C. Anderson, R. Rothlein, C. Lane, and P.R. Kvietys. 1992. Anoxia/reoxygenation-induced neutrophil adherence to cultured endothelial cells. *Am. J. Physiol.* 262:H1891–H1898.
23. Muller, W.A., S.A. Weigl, X. Deng, and D.M. Phillips. 1993. PECAM-1 is required for transendothelial migration of leukocytes. *J. Exp. Med.* 178:449–460.
24. Bogen, S., J. Pak, M. Garifallou, X. Deng, and W. Muller. 1994. Monoclonal antibody to murine PECAM-1 (CD31) blocks acute inflammation in vivo. *J. Exp. Med.* 179:1059–1064.
25. Vaporciyan, A.A., H.M. DeLisser, H.C. Yan, I.I. Mendiguren, S.R. Thom, M.L. Jones, P.A. Ward, and S.M. Albelda. 1993. Involvement of platelet-endothelial cell adhesion molecule-1 in neutrophil recruitment in vivo. *Science (Wash. DC).* 262:1580–1582.
26. Bogen, S.A., H.S. Baldwin, S.C. Watkins, S.M. Albelda, and A.K. Abbas. 1992. Association of murine CD31 with transmigrating lymphocytes following antigenic stimulation. *Am. J. Pathol.* 141:843–854.
27. Russell, R.G., M.P. Nasisse, H.S. Larsen, and B.T. Rouse. 1984. Role of T-lymphocytes in the pathogenesis of herpetic stromal keratitis. *Invest. Ophthalmol. Vis. Sci.* 25:938–944.
28. Ksander, B.R., and R.L. Hendricks. 1987. Cell-mediated immune tolerance to HSV-1 antigens associated with reduced susceptibility to HSV-1 corneal lesions. *Invest. Ophthalmol. Vis. Sci.* 28:1986–1993.
29. Metcalf, J.F., D.S. Hamilton, and R.W. Reichert. 1979. Herpetic keratitis in athymic (nude) mice. *Infect. Immun.* 26: 1164–1171.
30. Metcalf, J.F., and H.E. Kaufman. 1976. Herpetic stromal keratitis: evidence for cell-mediated immunopathogenesis. *Am. J. Ophthalmol.* 82:827–834.
31. Hendricks, R.L., R.J. Epstein, and T.M. Tumpey. 1989. The effect of cellular immune tolerance to HSV-1 antigens on the immunopathology of HSV-1 keratitis. *Invest. Ophthalmol. Vis. Sci.* 30:105–115.
32. Hendricks, R.L., M.S.P. Tao, and J.C. Glorioso. 1989. Alterations in the antigenic structure of two major HSV-1 glycoproteins, gC and gB, influence immune regulation and susceptibility to murine herpes keratitis. *J. Immunol.* 142:263–269.
33. Newell, C.K., S. Martin, D. Sendele, C.M. Mercadal, and B.T. Rouse. 1989. Herpes simplex virus-induced stromal keratitis: role of T-lymphocyte subsets in immunopathology. *J. Virol.* 63:769–775.
34. Hendricks, R.L., and T.M. Tumpey. 1991. Concurrent regeneration of T lymphocytes and susceptibility to HSV-1 corneal stromal disease. *Curr. Eye Res.* 10:47–53.
35. Newell, C.K., D. Sendele, and B.T. Rouse. 1989. Effects of $CD4^+$ and $CD8^+$ T-lymphocyte depletion on the induction and expression of herpes simplex stromal keratitis. *Reg. Immunol.* 2:366–369.
36. Doymaz, M.Z., and B.T. Rouse. 1992. Herpetic stromal keratitis: an immunopathologic disease mediated by $CD4^+$ T lymphocytes. *Invest. Ophthalmol. Vis. Sci.* 33:2165–2173.
37. Thornhill, M.H., U. Kyan-Aung, T.H. Lee, and D.O. Haskard. 1990. T cells and neutrophils exhibit differential adhesion to cytokine-stimulated endothelial cells. *Immunology.* 69:287–292.
38. Issekutz, T.B., J.M. Stoltz, and P. van der Meide. 1988. Lymphocyte recruitment in delayed-type hypersensitivity. The role of IFN-gamma. *J. Immunol.* 140:2989–2993.
39. Issekutz, A.C., and T.B. Issekutz. 1993. Quantitation and kinetics of blood monocyte migration to acute inflammatory

reactions, and IL-1 alpha, tumor necrosis factor-alpha, and IFN-gamma. *J. Immunol.* 151:2105–2115.
40. Springer, T.A. 1990. Adhesion receptors of the immune system. *Nature (Lond.).* 346:425–434.
41. Renkonen, R., P. Mattila, M.-L. Majuri, T. Paavonen, and O. Silvennoinen. 1992. IL-4 decreases IFN-γ-gamma-induced endothelial ICAM-1 expression by a transcriptional mechanism. *Scand. J. Immunol.* 35:525–530.
42. Carlos, T.M., B.R. Schwartz, N.L. Kovach, E. Yee, M. Rosa, L. Osborn, G. Chi-Rosso, B. Newman, and R. Lobb. 1990. Vascular cell adhesion molecule-1 mediates lymphocyte adherence to cytokine-activated cultured human endothelial cells. *Blood.* 76:965–970.
43. Dustin, M.L., R. Rothlein, A.K. Bhan, C.A. Dinarello, and T.A. Springer. 1986. Induction by IL-1 and interferon-gamma: tissue distribution, biochemistry, and function of a natural adherence molecule (ICAM-1). *J. Immunol.* 137: 245–254.
44. Kurose, I., C. Pothoulakis, J.T. LaMont, D.C. Anderson, J.C. Pauson, M. Miyasaka, R. Wolf, and D.N. Granger. 1994. *Clostridium difficile* toxin A-induced microvascular dysfunction. Role of histamine. *J. Clin. Invest.* 94:1919–1926.
45. Wallace, J.L., W. McKnight, M. Miyasaka, T. Tamatani, J. Paulson, D.C. Anderson, D.N. Granger, and P. Kubes. 1993. Role of endothelial adhesion molecules in NSAID-induced gastric mucosal injury. *Am. J. Physiol.* 265:G993–G998.
46. Issekutz, A.C., and T.B. Issekutz. 1993. A major portion of polymorphonuclear leukocyte and T lymphocyte migration to arthritic joints in the rat is via LFA-1/MAC-1-independent mechanisms. *Clin. Immunol. Immunopathol.* 67:257–263.
47. Munro, J.M., J.S. Pober, and R.S. Cotran. 1991. Recruitment of neutrophils in the local endotoxin response: association with de novo endothelial expression of endothelial leukocyte adhesion molecule-1. *Lab. Invest.* 64:295–299.
48. Staats, H.F., and R.N. Lausch. 1993. Cytokine expression in vivo during murine herpetic stromal keratitis. *J. Immunol.* 151:277–283.
49. Favaloro, E.J. 1993. Differential expression of surface antigens on activated endothelium. *Immunol. Cell Biol.* 71:571–581.
50. Romer, L.H., N.V. McLean, H.-C. Yan, M. Daise, J. Sun, and H.M. DeLisser. 1995. IFN-γ and TNF-α induce redistribution of PECAM-1 (CD31) on human endothelial cells. *J. Immunol.* 154:6582–6592.
51. DeLisser, H.M., P.J. Newman, and S.M. Albelda. 1994. Molecular and functional aspects of PECAM-1/CD31. *Immunol. Today.* 15:490–495.
52. Berger, R., S.M. Albelda, D. Berd, M. Ioffreda, D. Whitaker, and G.F. Murphy. 1993. Expression of platelet-endothelial cell adhesion molecule-1 (PECAM-1) during melanoma-induced angiogenesis in vivo. *J. Cutan. Pathol.* 20:399–406.
53. Liao, F., H.K. Huynh, A. Eiroa, T. Greene, E. Polizzi, and W.A. Muller. 1995. Migration of monocytes across endothelium and passage through extracellular matrix involve separate molecular domains of PECAM-1. *J. Exp. Med.* 182: 1337–1343.
54. Wakelin, M.W., M.-J. Sanz, A. Dewar, S.M. Albelda, S.W. Larkin, N. Boughton-Smith, T.J. Williams, and S. Nourshargh. 1996. An anti–platelet–endothelial cell adhesion molecule-1 antibody inhibits leukocyte extravasation from mesenteric microvessels in vivo by blocking the passage through the basement membrane. *J. Exp. Med.* 184:229–239.